

# Size truncation effect, threshold behavior, and a new type of autoconversion parameterization

Yangang Liu, Peter H. Daum, and Robert L. McGraw

Atmospheric Sciences Division, Brookhaven National Laboratory, Upton, New York, USA

Received 4 February 2005; revised 2 April 2005; accepted 10 May 2005; published 15 June 2005.

[1] A function defined as the size truncation function is introduced to quantify the effect of truncating the cloud droplet size distribution on the autoconversion rate. It is shown that the size truncation function can be used as a threshold function to represent the threshold behavior associated with the autoconversion process, providing a physical basis for the threshold function. Comparisons of the new threshold function with those ad hoc threshold functions associated with existing Kessler-type and Sundqvist-type parameterizations reveals the degree of approximations of the two empirical parameterizations. Application of the new threshold function leads to a new type of autoconversion parameterization that is fully analytical, physics-based, and removes the ad hoc nature of threshold representation in existing autoconversion parameterizations. **Citation:** Liu, Y., P. H. Daum, and R. L. McGraw (2005), Size truncation effect, threshold behavior, and a new type of autoconversion parameterization, *Geophys. Res. Lett.*, 32, L11811, doi:10.1029/2005GL022636.

## 1. Introduction

[2] Accurate representation of microphysical processes is crucial for improving cloud-resolving models and global climate models [Cotton and Anthes, 1989; Stokes and Schwartz, 1994]. A key microphysical process that needs to be parameterized is autoconversion whereby cloud droplets collect each other and become embryonic raindrops [Kessler, 1969; Manton and Cotton, 1977; Liou and Ou, 1989; Baker, 1993; Liu and Daum, 2004]. As the first step from cloud to rain, accurate parameterization of the autoconversion process is especially important for estimating the second indirect aerosol effect [Boucher *et al.*, 1995; Lohmann and Fleichter, 1997; Rotstajn, 2000; Rotstajn and Liu, 2005].

[3] All the autoconversion parameterizations that have been developed so far can be generically written as

$$P = P_0 T, \quad (1)$$

where  $P$  is the autoconversion rate;  $P_0$  represents the conversion rate after the onset of the autoconversion process (rate function hereafter), and  $T$  represents the threshold function describing the threshold behavior of the autoconversion process. The rate function  $P_0$  has been the primary focus of previous studies, and great progress has been made over the last few decades [Kessler, 1969; Manton and Cotton, 1977; Liou and Ou, 1989; Baker,

1993; Liu and Daum, 2004]. See Liu and Daum [2004] also for discussions and comparisons of different rate functions.

[4] The threshold function  $T$ , however, has received little attention. The only two available expressions are ad hoc in nature [Kessler, 1969; Sundqvist, 1978; Del Genio *et al.*, 1996] (see Section 2 for more discussions). Some simulation-based parameterizations obtained by fitting simulations of detailed microphysical models implicitly assume  $T = 1$  [Beheng, 1994; Khairoutdinov and Kogan, 2000], which can be considered as a special case. Lack of physics behind these ad hoc threshold functions is a deficiency of existing autoconversion parameterizations, precluding a sound choice between these ad hoc threshold functions. Another deficiency is that many autoconversion parameterizations implicitly include cloud droplets of all sizes in calculation of the autoconversion rate. This assumption is incorrect because the autoconversion process as defined occurs only over a certain range of droplet sizes. The effect on the autoconversion rate due to the neglect of the truncation of the cloud droplet size distribution (size truncation effect) has not been well addressed.

[5] As an extension of our two recent studies that derive theoretical expressions for the rate function [Liu and Daum, 2004] and the critical radius associated with the Kessler-type parameterizations [Liu *et al.*, 2004], the objective of this work is to theoretically derive a threshold function, and to show that threshold behavior and the size truncation effect can be equivalently treated. We further show that the new threshold function is an analytical function of the liquid water content ( $L$ ) and the droplet concentration ( $N$ ). Combining the new threshold function with the Liu-Daum rate function leads to a new type of parameterization that removes many deficiencies of existing autoconversion parameterizations.

## 2. Existing Threshold Functions

[6] Existing autoconversion parameterizations can be classified as Kessler-type or Sundqvist-type according to the way of specifying threshold function  $T$ . Briefly, Kessler [1969] assumed that the autoconversion process exhibits a threshold behavior as described by a Heaviside step function,

$$T_K = H(L - L_c), \quad (2a)$$

where  $H(L - L_c)$  is the Heaviside step function indicating no autoconversion when  $L$  is less than the threshold value  $L_c$ . Later Kessler-type parameterizations [Manton and Cotton, 1977; Liou and Ou, 1989; Baker, 1993; Liu and

Daum, 2004] replace  $L$  with a measure of droplet size such that

$$T_K = H(r_m - r_c), \quad (2b)$$

where  $r_m$  and  $r_c$  denotes the driving and critical radii, respectively. Although it has been agreed that the threshold process in Kessler-type parameterizations is driven by some kind of mean radius, the definition of  $r_m$  differs for different Kessler-type parameterizations. For example,  $r_m$  respectively represents the mean radius of the third moment ( $r_3$ ) in the parameterization of *Manton and Cotton* [1977], mean radius of the fourth moment ( $r_4$ ) in the parameterizations of *Liou and Ou* [1989], *Baker* [1993] and *Boucher et al.* [1995], and mean radius of the sixth moment ( $r_6$ ) in *Liu and Daum* [2004]. Furthermore,  $r_c$  had been tuned in modeling studies until recently when *Liu et al.* [2004] related  $r_c$  to  $L$  and  $N$  based on the kinetic potential theory formulated by *McGraw and Liu* [2003, 2004]. The kinetic potential theory also provides a physical basis for considering the autoconversion process as a threshold process.

[7] *Sundqvist* [1978] proposed another ad hoc threshold function,

$$T_S = 1 - \exp\left[-\left(\frac{L}{L_c}\right)^2\right]. \quad (2c)$$

*Del Genio et al.* [1996] introduced a slightly different threshold function

$$T_S = 1 - \exp\left[-\left(\frac{L}{L_c}\right)^4\right]. \quad (2d)$$

Equation (2d) exhibits a cloud-to-rain transition sharper than equation (2c), but still smoother than the Heaviside function. Sundqvist-type parameterizations have been recently generalized to explicitly consider  $N$  and relative dispersion (Y. Liu, et al., Parameterization of the autoconversion process. part II: Generalization of Sundqvist-type parameterizations, submitted to *Journal of the Atmospheric Sciences*, 2005). The generalized Sundqvist threshold function is given by

$$T_S = 1 - \exp\left[-\left(\frac{\bar{m}}{m_c}\right)^\mu\right] = 1 - \exp\left[-\left(\frac{r_3}{r_c}\right)^{3\mu}\right], \quad (2e)$$

where  $\bar{m} = L/N$  is the mean mass, and  $m_c = L_c/N$  is the critical mass. The exponent  $\mu \geq 0$  is introduced to unify Kessler and Sundqvist-type parameterizations. The latter approaches the former when  $\mu$  approaches  $\infty$ . However, there is no physical basis for any of these threshold functions.

### 3. New Type of Autoconversion Parameterization

#### 3.1. Liu-Daum Rate Function

[8] Here we recapitulate the derivation of the rate function presented in *Liu and Daum* [2004] for later use. The mass growth rate of a collector drop of radius  $r$  falling

through a population of droplets having a cloud droplet size distribution  $n(R)$  is given by [*Pruppacher and Klett*, 1997]

$$\frac{dm(r)}{dt} = \frac{4\pi\rho_w}{3} \int K(r, R)R^3 n(R) dR, \quad (3)$$

where  $K(r, R)$  is the collection kernel and  $\rho_w$  is the water density. The autoconversion rate is obtained by further integrating equation (3) over all collector drops:

$$P_{LH} = \int \frac{dm}{dt} n(r) dr = \frac{4\pi\rho_w}{3} \int \int n(r) \cdot K(r, R)R^3 n(R) dr dR \quad (4)$$

Application of the Long kernel [*Long*, 1974] for  $r < 50 \mu\text{m}$  [ $K(r, R) = \kappa_2 r^6$ , where  $\kappa_2 \approx 1.9 \times 10^{11}$  is in  $\text{cm}^{-3} \text{s}^{-1}$ ,  $r$  is in  $\text{cm}$ , and  $K$  is in  $\text{cm}^3 \text{s}^{-1}$ ] yields

$$P_{LH} = \kappa\beta^6 N^{-1} L^3, \quad (5)$$

where  $\kappa = \left(\frac{3}{4\pi\rho_w}\right)^2 \kappa_2 = 1.1 \times 10^{10}$  ( $\text{g}^{-2} \text{cm}^3 \text{s}^{-1}$ ), and  $\beta$  depends on the relative dispersion.

#### 3.2. Size Truncation Effect and a New Threshold Function

[9] All the above equations hold when truncating the cloud droplet size distribution between  $r_c$  and  $r_d$  ( $r_d$  is the upper truncation radius), except that equation (5) becomes

$$P = \kappa\beta_e^6 N_e^{-1} L_e^3, \quad (6a)$$

$$N_e = \int_{m_c}^{m_d} n(m) dm, \quad (6b)$$

$$L_e = \int_{m_c}^{m_d} mn(m) dm, \quad (6c)$$

$$\beta_e = \frac{\left[\int_{m_c}^{m_d} m^2 n(m) dm\right]^{1/6} \left[\int_{m_c}^{m_d} mn(m) dm\right]^{-1/3}}{\left[\int_{m_c}^{m_d} n(m) dm\right] \left[\int_{m_c}^{m_d} n(m) dm\right]}, \quad (6d)$$

where  $m_d$  is the upper truncation mass. Introducing the size truncation function  $\alpha$  defined as

$$\alpha = \alpha_\beta^6 \alpha_N^{-1} \alpha_L^3, \quad (7a)$$

where  $\alpha_y = y/y_e$  ( $y \equiv \beta, N$ , and  $L$ ), we can conveniently rewrite equation (6a) as

$$P = \alpha\kappa\beta^6 N^{-1} L^3 = \alpha P_{LH}. \quad (7b)$$

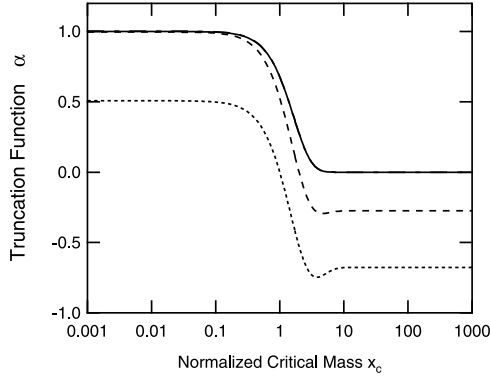


**Figure 1.** Size truncation effect as a function of the normalized critical mass  $x_c$ .

To evaluate  $\alpha$ , we employ a typical exponential mass distribution (see *Liu et al.* [1995], *Liu and Hallett* [1997], and *Costa et al.* [2000] for justification of using this distribution),

$$n(m) = \frac{N}{\bar{m}} \exp\left(-\frac{m}{\bar{m}}\right). \quad (8)$$

Substitution of equation (8) into equations (6b, 6c, 6d) yields the following expressions:

$$\alpha_N = e^{-x_c} - e^{-x_d}, \quad (9a)$$

$$\alpha_L = [(x_c + 1)e^{-x_c} - (x_d + 1)e^{-x_d}], \quad (9b)$$

$$\alpha_\beta^6 = \frac{1}{2} \frac{[(x_c^2 + 2x_c + 2)e^{-x_c} - (x_d^2 + 2x_d + 2)e^{-x_d}](e^{-x_c} - e^{-x_d})}{[(1 + x_c)e^{-x_c} - (1 + x_d)e^{-x_d}]^2}, \quad (9c)$$

$$\alpha = \frac{1}{2} \frac{[(x_c^2 + 2x_c + 2)e^{-x_c} - (x_d^2 + 2x_d + 2)e^{-x_d}]}{[(1 + x_c)e^{-x_c} - (1 + x_d)e^{-x_d}]} \quad (9d)$$

where the normalized upper truncation mass  $x_d = \frac{m_d}{\bar{m}}$ , and the normalized critical mass  $x_c = \frac{m_c}{\bar{m}}$ . According to equation (9d), for a given  $x_d$ ,  $\alpha$  is a unique function of  $x_c$ . When  $x_d = \infty$ , equation (9d) becomes

$$\alpha_\infty = \frac{1}{2} (x_c^2 + 2x_c + 2)(1 + x_c)e^{-2x_c} \quad (9e)$$

[10] Figure 1 shows  $\alpha$  as a function of  $x_c$  for  $x_d = 1$  (dotted), 2 (dashed), 10 (dot-dashed), and  $\infty$  (solid), respectively. It is clear from Figure 1 that  $\alpha$  quickly approaches  $\alpha_\infty$  after  $x_d$  approaches 10 (Note that the dot-dashed curve for  $x_d = 10$  overlaps the solid curve for  $\alpha_\infty$ ). Because the condition that  $x_d = 10$ , or  $r_d = 10^{1/3}r_3$ , is usually satisfied (e.g.,  $x_d = 37$  if  $r_d = 50 \mu\text{m}$  and  $r_3 = 15 \mu\text{m}$ ), it is reasonable to assume that  $\alpha = \alpha_\infty$ . Furthermore,  $\alpha_\infty$  exhibits the threshold behavior expected for the threshold function.

The equivalence of the size truncation function and the threshold function is evident from that  $r_c$  signals the onset of the autoconversion process. For consistency with equation (1),  $\alpha_\infty$  is hereafter referred to as the new threshold function and denoted as  $T_{\text{New}}$ .

[11] The new threshold function  $T_{\text{New}}$  provides a unified explanation for, and sheds light on the approximations of the commonly used ad hoc Kessler and Sundqvist threshold functions. Figure 2 compares  $T_{\text{New}}$  (black) with the Kessler (green) and Sundqvist (red) threshold functions. The solid and dashed red curves denote the curves calculated from equation (2e) with two commonly used values of  $\mu = 2, 4$ , respectively. It is clear from Figure 2 that the two typical Sundqvist-type threshold functions approximate  $T_{\text{new}}$  better than the step function.

### 3.3. Analytical Expression for $x_c$ and the New Parameterization

[12] Based on the kinetic potential theory on drizzle formation, *Liu et al.* [2004] derived an analytical expression that relates  $r_c$  to  $L$  and  $N$ ,

$$r_c = \left(\frac{3}{4\pi}\right)^{1/3} \frac{\nu^{1/3} \beta_{\text{con}}^{1/6}}{\kappa^{1/6}} N^{1/6} L^{-1/3}, \quad (10)$$

where  $\nu = 3.0 \times 10^{-23}$  (g), and  $\beta_{\text{con}} = 1.15 \times 10^{23}$  ( $\text{s}^{-1}$ ). See also *McGraw and Liu* [2004] for an alternative derivation of equation (10). The critical mass and  $x_c$  are then given by equations (11) and (12), respectively:

$$m_c = \left(\frac{4\pi\rho_w}{3}\right) r_c^3 = \frac{\rho_w \nu}{\kappa^{1/2}} \beta_{\text{con}}^{1/2} N^{1/2} L^{-1}, \quad (11)$$

$$x_c = \frac{m_c}{\bar{m}} = \frac{\rho_w \nu}{\kappa^{1/2}} \beta_{\text{con}}^{1/2} N^{3/2} L^{-2} = 9.7 \times 10^{-17} N^{3/2} L^{-2}. \quad (12)$$

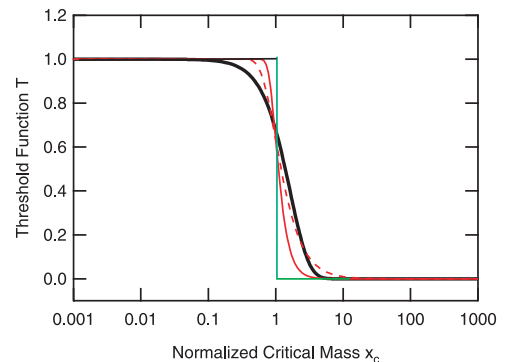


**Figure 2.** Comparison of the new threshold function (black solid) with the Kessler-type threshold function (green solid) and the Sundqvist-type threshold function with  $\mu = 2$  (red dotted), and  $\mu = 4$  (red solid). In general, let the driving radius  $r_m = \beta r_3$ , then the identity  $r_m = r_c$  leads to  $r_c/r_3 = \beta$ , or  $x_c = \beta^3$ . Therefore, changing from  $r_m = r_3$  to  $r_4, r_6$  means shifting  $x_c$  to the right ( $\beta > 1$ ), and the amount of shift depends on the relative dispersion.

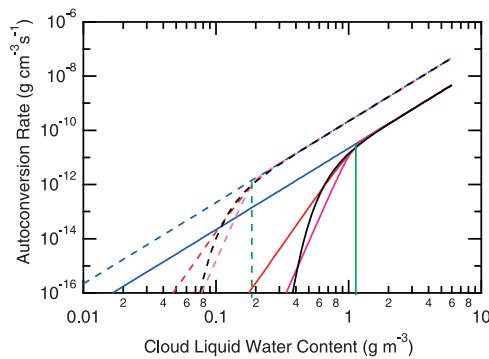


**Figure 3.** Comparison of the new type of autoconversion parameterization with existing ones. The dashed and solid curves represent that for  $N = 50 \text{ cm}^{-3}$  and  $N = 500 \text{ cm}^{-3}$ , respectively. The black, green, red and purple colors represent results from the new parameterization, the Kessler-type parameterization with  $r_3$  as the driving radius, and the Sundqvist-type parameterizations with  $\mu = 2, 4$ , respectively. The blue cover simply represents the Liu-Daum rate function. The  $L_c$  values ( $L_c = 0.19 \text{ gm}^{-3}$  for  $N = 50 \text{ cm}^{-3}$ ;  $L_c = 1.04 \text{ gm}^{-3}$  for  $N = 500 \text{ cm}^{-3}$  are determined by setting  $x_c = 1$  in equation (12) such that  $L_c = 9.8 \times 10^{-9} N^{3/4}$ .

Substitution of equations (12) and (9e) into equation (7b) yields a new type of autoconversion parameterization that is an analytical function of  $L$  and  $N$ .

#### 4. Further Examination

[13] This section provides further comparisons of the new type of autoconversion parameterization against the two ad hoc types that have been widely used. Figure 3 shows the autoconversion rate as a function of  $L$  for  $N = 50 \text{ cm}^{-3}$  (dashed) and  $N = 500 \text{ cm}^{-3}$  (solid), respectively. The black line represent results from the new parameterization, red line the Kessler-type parameterization with  $r_3$  as the driving radius, and green and purple lines the Sundqvist-type parameterizations with  $\mu = 2, 4$ , respectively. The blue line represents the Liu-Daum rate function. It is evident from Figure 3 that all the parameterizations give almost the same autoconversion rates as the rate function beyond the autoconversion threshold. The autoconversion threshold manifests itself as steep fall when  $L$  is less than some threshold  $L_c$ . This is similar to that originally conceived by Kessler [1969]. However,  $L_c$  increases with increasing  $N$  instead of being a constant as assumed by Kessler. Furthermore, examination of the different curves reveals that Sundqvist-type parameterizations with smooth transitions approximate the new theoretical autoconversion rate better than the corresponding Kessler-type parameterizations.

#### 5. Concluding Remarks

[14] It is shown that the threshold behavior associated with the autoconversion process can be represented by the size truncation function, providing a physical explanation for the threshold function. A new type of parameterization is obtained by coupling the new threshold function with our recently derived expressions for the rate function and

critical radius. The new autoconversion parameterization further reveals the approximations and eliminates many deficiencies of existing Kessler-type and Sundqvist-type parameterizations. For example, in contrast to Kessler-type parameterizations, new parameterization does not require specification of the driving radius and critical radius. Furthermore, it is shown that Sundqvist-type parameterizations with smooth cloud-to-rain transitions describe the autoconversion rate better than Kessler-type parameterizations with discontinuously sharp transition. The fact that the autoconversion rate is a product of the rate function and the threshold function also raises questions as to those parameterizations based on fitting numerical results from detailed microphysical simulations with a simple function.

[15] Three unique features of the new autoconversion parameterization are worth emphasizing. First, this parameterization appears to be the first that theoretically integrates the threshold behavior of the autoconversion process (or size truncation effect) into the expression for the autoconversion rate. Second, its application in atmospheric models should require no more effort than existing parameterizations. Finally, unlike existing parameterizations, the new parameterization does not have tunable parameters, but is instead fully determined by physics.

[16] **Acknowledgments.** This research was supported by the DOE Atmospheric Radiation Measurements Program and Atmospheric Sciences Program. The authors thank Drs. Rotstayn at CSIRO, Ghan at PNL and an anonymous reviewer for their insightful comments. This manuscript has been authored by Brookhaven Science Associates, LLC under Contract No. DE-AC02-98CH1-886 with the U.S. Department of Energy. The United States Government retains, and the publisher, by accepting the article for publications, acknowledges, a world-wide license to publish or reproduce the published form of this manuscript, or allow others to do so, for the United States Government purposes.

#### References

- Baker, M. B. (1993), Variability in concentrations of CCN in the marine cloud-top boundary layer, *Tellus, Ser. B*, 45, 458–472.
- Beheng, K. D. (1994), A parameterization of warm cloud microphysical conversion processes, *Atmos. Res.*, 33, 193–206.
- Boucher, O., H. L. Treut, and M. B. Baker (1995), Precipitation and radiation modeling in a general circulation model: Introduction of cloud microphysical process, *J. Geophys. Res.*, 100(D8), 16,395–16,414.
- Costa, A., C. Oliveira, J. Oliveira, and A. Sampaio (2000), Microphysical observations of warm cumulus clouds in Ceara, Brazil, *Atmos. Res.*, 54, 167–199.
- Cotton, W. R., and R. A. Anthes (1989), *Storms and Cloud Dynamics*, 883 pp., Elsevier, New York.
- Del Genio, A. D., M. Yao, W. Kovari, and K. K. Lo (1996), A prognostic cloud water parameterization for climate models, *J. Clim.*, 9, 270–304.
- Kessler, E. (1969), On the distribution and continuity of water substance in atmospheric circulation, *Meteorol. Monogr.*, 10, 84 pp.
- Khairoutdinov, M., and Y. Kogan (2000), A new cloud physics parameterization in a large-eddy simulation model of marine stratocumulus, *Mon. Weather Rev.*, 128, 229–243.
- Liou, K. N., and S. C. Ou (1989), The role of cloud microphysical processes in climate: An assessment from a one-dimensional perspective, *J. Geophys. Res.*, 94(D6), 8599–8607.
- Liu, Y., and P. H. Daum (2004), Parameterization of the autoconversion process. part I: Analytical formulation of the Kessler-type parameterizations, *J. Atmos. Sci.*, 61, 1539–1548.
- Liu, Y., and J. Hallett (1997), The “1/3” power-law between effective radius and liquid water content, *Q. J. R. Meteorol. Soc.*, 123, 1789–1795.
- Liu, Y., L. You, W. Yang, and F. Liu (1995), On the size distribution of cloud droplets, *Atmos. Res.*, 35, 201–216.
- Liu, Y., P. H. Daum, and R. McGraw (2004), An analytical expression for predicting the critical radius in the autoconversion parameterization, *Geophys. Res. Lett.*, 31, L06121, doi:10.1029/2003GL019117.
- Lohmann, U., and J. Fleichter (1997), Impact of sulfate aerosols on albedo and lifetime of clouds: A sensitivity study with the ECHAM 4 GCM, *J. Geophys. Res.*, 102(D12), 13,685–13,700.

- Long, A. B. (1974), Solutions to the droplet collection equation for polynomial kernels, *J. Atmos. Sci.*, *31*, 1040–1052.
- Manton, M. J., and W. R. Cotton (1977), Formulation of approximate equations for modeling moist deep convection on the mesoscale, *Atmos. Sci. Pap.* *266*, Dep. of Atmos. Sci., Colo. State Univ., Fort Collins.
- McGraw, R., and Y. Liu (2003), Kinetic potential and barrier crossing: A model for warm cloud drizzle formation, *Phys. Rev. Lett.*, *90*, 018501, doi:10.1103/PhysRevLett.90.018501.
- McGraw, R., and Y. Liu (2004), Analytical formulation and parameterization of the kinetic potential theory for drizzle formation, *Phys. Rev. E*, *70*, 031606, doi:10.1103/PhysRevE.70.031606.
- Pruppacher, H. R., and J. D. Klett (1997), *Microphysics of Clouds and Precipitation*, 954 pp., Springer, New York.
- Rotstajn, L. D. (2000), On the “tuning” of the autoconversion parameterizations in climate models, *J. Geophys. Res.*, *105*(D12), 15,495–15,507.
- Rotstajn, L. D., and Y. Liu (2005), A smaller global estimate of the second indirect aerosol effect, *Geophys. Res. Lett.*, *32*, L05708, doi:10.1029/2004GL021922.
- Stokes, G. M., and S. E. Schwartz (1994), The Atmospheric Radiation Measurement (ARM) Program: Programmatic background and design of the cloud and radiation test bed, *Bull. Am. Meteorol. Soc.*, *75*, 1201–1221.
- Sundqvist, H. (1978), A parameterization scheme for non-convective condensation including prediction of cloud water content, *Q. J. R. Meteorol. Soc.*, *104*, 677–690.
- 
- P. H. Daum, Y. Liu, and R. L. McGraw, Atmospheric Sciences Division, Brookhaven National Laboratory, Building 815E, Upton, NY 11973-5000, USA. (phdaum@bnl.gov; lyg@bnl.gov; rlm@bnl.gov)